Direct Methods for Reconstruction of Functions and their Edges from Non-Uniform Fourier Data

Aditya Viswanathan
aditya@math.msu.edu

MICHIGAN STATE UNIVERSITY

ICERM Research Cluster
Computational Challenges in Sparse and Redundant Representations
$17^{\mathtt{th}}$ November 2014

Outline

Model Problem

Let f be defined in $\mathbb{R}$ with support in $[-\pi, \pi)$. Given

$$\hat{f}(\omega_k) = \left\langle f, e^{i\omega_k x} \right\rangle, \quad k = -N, \cdots, N,$$

(ω_k not necessarily $\in \mathbb{Z}$)

compute

- an approximation to the underlying function f,
- an approximation to the locations and values of jumps in the underlying function; i.e.,

$$[f](x) := f(x^+) - f(x^-).$$

Motivating Application – Magnetic Resonance Imaging

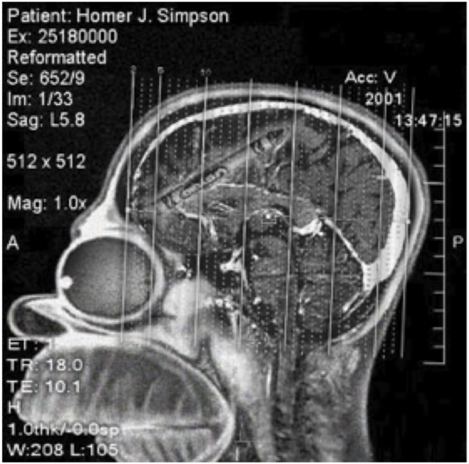

Physics of MRI dictates that the MR scanner collect samples of the Fourier transform of the specimen being imaged.

Motivating Application – Magnetic Resonance Imaging

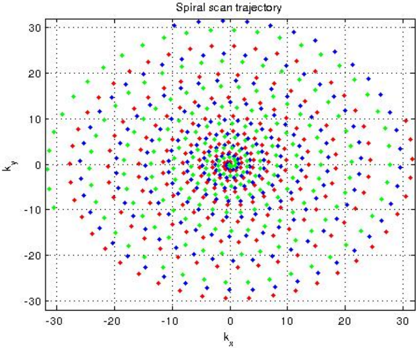

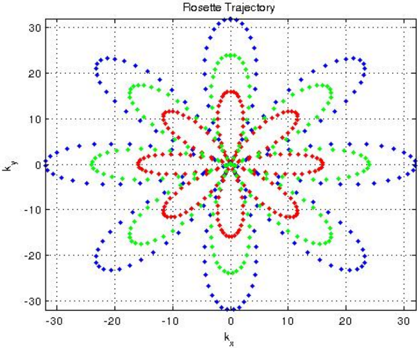

- Collecting non-uniform measurements has certain advantages; for example, they are easier and faster to collect, and, aliased images retain diagnostic qualities.

Challenges in Non-Uniform Reconstruction

- *Computational Issues*
  - The FFT is not directly applicable.
  - Direct versus iterative solvers ...
- *Sampling Issues*
  Typical MR sampling patterns have non uniform sampling density; i.e., the high modes are sparsely sampled ($|\omega_k - k| > 1$ for k large).
- *Other Issues*
  Piecewise-smooth functions and Gibbs artifacts

Why Direct Methods?

- Faster (by a small but non-negligible factor) than iterative formulations.
- Provide good initial solutions to seed iterative algorithms.
- Sometimes used as preconditioners in solving iterative formulations.

Model (1D) Sampling Patterns

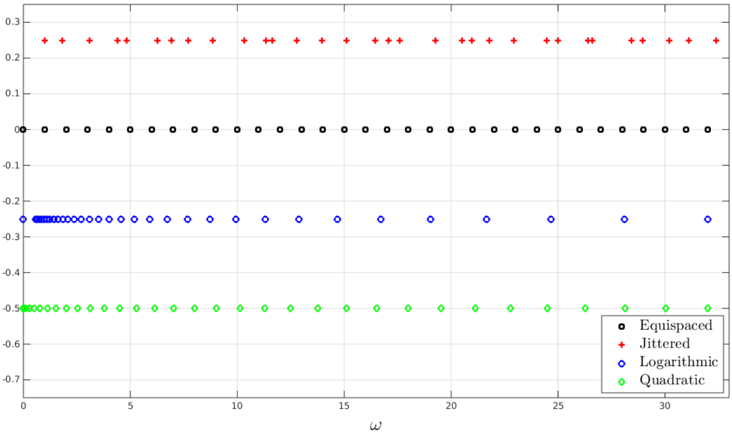

Jittered Sampling: $\omega_k = k \pm U[0, \mu], \quad k = -N, \cdots, N$

$U[a, b]$: iid uniform distribution in $[a, b]$ with equiprobable $+/-$ jitter.

Model (1D) Sampling Patterns

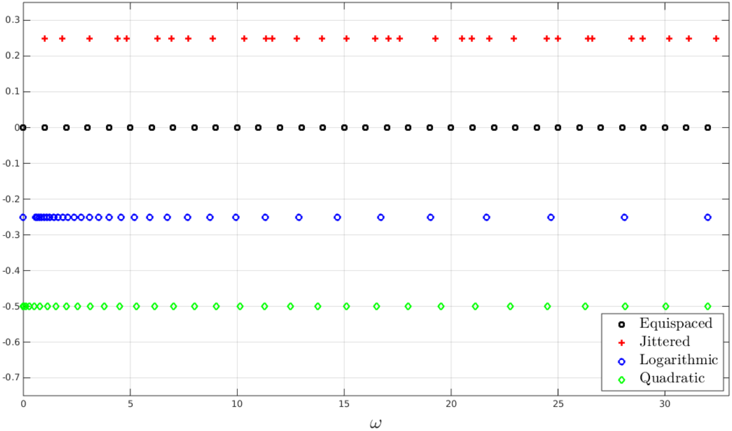

Log Sampling: $$\omega_{k+} = a\, e^{b(2\pi k)}, \quad k = 1, \ldots, N, \quad b = \frac{\ln(N/a)}{2\pi N}$$

a controls the closest sampling point to the origin.

Model (1D) Sampling Patterns

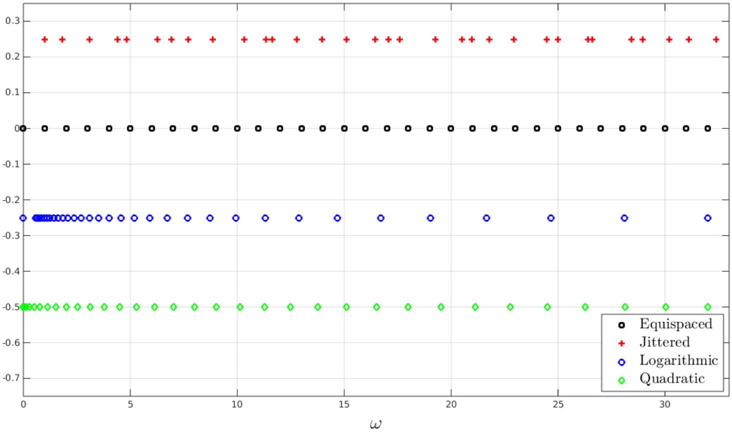

Polynomial Sampling: $\omega_{k+} = a\, k^b, \quad k = 1, \ldots, N, \quad a = \dfrac{1}{N^{b-1}}$

b is the polynomial order.

Outline

Uniform Re-Sampling (Rosenfeld[1])

Consider a two step reconstruction process:

1. Approximate the Fourier coefficients at equispaced modes
2. Compute a standard (filtered) Fourier partial sum

<u>Basic Premise</u>
f is compactly supported in physical space. Hence, the *Shannon sampling theorem* is applicable in Fourier space; i.e.,

$$\hat{f}(\omega) = \sum_{k=-\infty}^{\infty} \mathrm{sinc}(\omega - k)\hat{f}_k, \quad \omega \in \mathbb{R}.$$

[1] *An optimal and efficient new gridding algorithm using singular value decomposition*, D. Rosenfeld, Magn Reson Med. 1998 Jul;40(1):14–23.

Uniform Re-Sampling – Implementation

We truncate the problem as follows

$$\hat{f}(\omega_k) \approx \sum_{|\ell|\leq M} \mathsf{sinc}(\omega_k - \ell)\hat{f}_\ell, \quad k = -N, \cdots, N$$

$$\underbrace{\begin{bmatrix} \hat{f}(\omega_{-N}) \\ \cdot \\ \cdot \\ \cdot \\ \hat{f}(\omega_N) \end{bmatrix}}_{\text{measurements } \hat{\mathbf{f}}} \approx \underbrace{\begin{bmatrix} \mathsf{sinc}(\omega_{-N} + M) & \ldots & \mathsf{sinc}(\omega_{-N} - M) \\ \cdot & \ldots & \ldots \\ \cdot & \ldots & \ldots \\ \cdot & \ldots & \ldots \\ \mathsf{sinc}(\omega_N + M) & \ldots & \mathsf{sinc}(\omega_N - M) \end{bmatrix}}_{\text{Sampling system matrix } A \in \mathbb{R}^{2N+1 \times 2M+1}} \underbrace{\begin{bmatrix} \hat{f}(\omega_{-M}) \\ \cdot \\ \cdot \\ \cdot \\ \hat{f}(\omega_M) \end{bmatrix}}_{\text{re-sampled coefficients } \bar{\mathbf{f}}}$$

Uniform Re-Sampling – Implementation

The (equispaced) re-sampled coefficients are approximated as

$$\bar{\mathbf{f}} = A^{\dagger}\hat{\mathbf{f}},$$

where $A^{\dagger}$ is the Moore-Penrose pseudo-inverse of A.

- A and its properties characterize the resulting approximation.
- Regularization may be used (truncated SVD, Tikhonov regularization) in the presence of noise.
- $A^{\dagger}$ is a dense matrix in general. A block variant of this method exists (Block Uniform Re-Sampling, which constructs a sparse $A^{\dagger}$.

Uniform Re-sampling – Examples

Reconstruction from Polynomial (quadratic) samples.

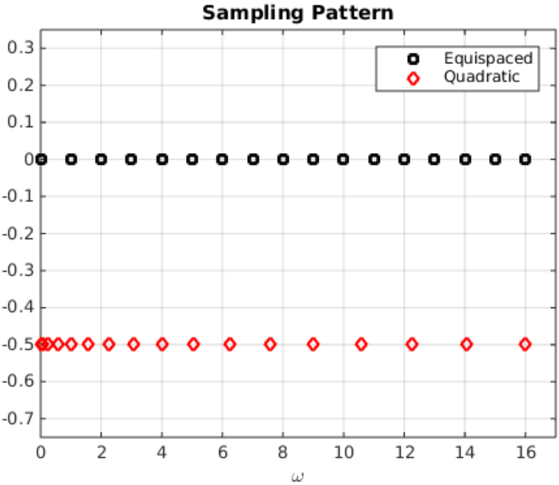

Uniform Re-sampling – Examples

Reconstruction from Polynomial (quadratic) samples.

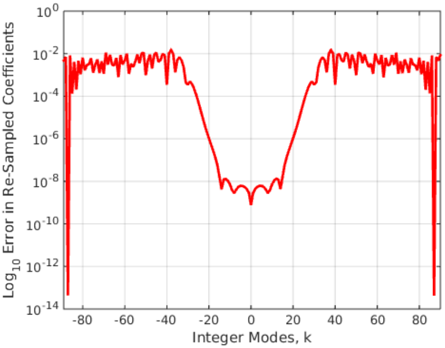

Error – Fourier Modes

Reconstruction

Uniform Re-sampling – Examples

Reconstruction from Polynomial (quadratic) samples.

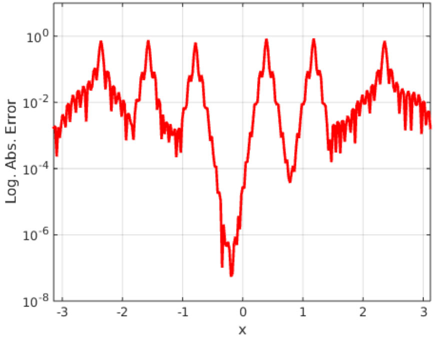

Reconstruction Error

Reconstruction

Further Reading

- *New Approach to Gridding using Regularization and Estimation Theory*, D. Rosenfeld, Magn Reson Med. 2002; 48:193–202
- *Applying the uniform resampling (URS) algorithm to a Lissajous trajectory: Fast image reconstruction with optimal gridding*, Moriguchi H., Wendt M., Duerk JL., Magn Reson Med. 2000; 44:766–781

From Uniform Re-sampling to Convolutional Gridding

Recall that for uniform re-sampling, we use the relation

$$\hat{f}(\omega) = \sum_k \mathsf{sinc}(\omega - k)\hat{f}_k = (\hat{f} * \mathsf{sinc})(\omega)$$

Since the Fourier transform pair of the sinc function is the box/rect function (of width 2π and centered at zero), we have

$$f \cdot \Pi \longleftrightarrow \hat{f} * \mathsf{sinc}$$

Now consider replacing the sinc function by a bandlimited function $\hat{\phi}$ such that $\hat{\phi}(|\omega|) = 0$ for $|\omega| > q$ (typically a few modes wide). We now have

$$f \cdot \phi \longleftrightarrow \hat{f} * \hat{\phi}$$

Convolutional Gridding (Jackson/Meyer/Nishimura . . .)

- Gridding is an inexpensive *direct* approximation to the uniform re-sampling procedure.
- Given measurements $\hat{f}(\omega_k)$, we compute an approximation to $\hat{f} * \hat{\phi}$ at the equispaced modes using

$$(\hat{f} * \hat{\phi})(\ell) \approx \sum_{|\ell - \omega_k| \leq q} \alpha_k \hat{f}(\omega_k) \hat{\phi}(\ell - \omega_k), \quad \ell = -M, \ldots, M.$$

- α_k are desity compensation factors (DCFs) and determine the accuracy of the reconstruction.

Convolutional Gridding (Jackson/Meyer/Nishimura . . .)

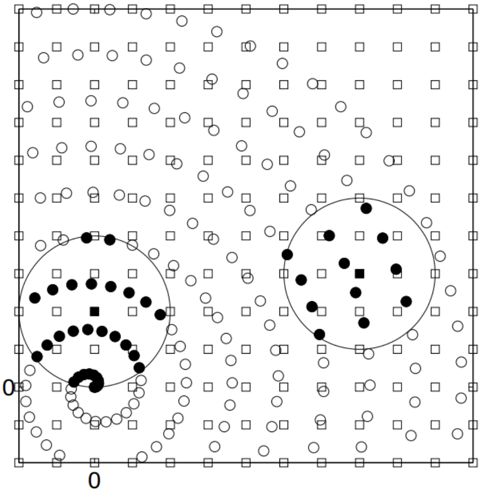

Figure : Gridding to a Cartesian Grid[3]

[3]http://web.eecs.umich.edu/ fessler/papers/files/talk/06/isbi,p2,slide,bw.pdf

Convolutional Gridding (Jackson/Meyer/Nishimura ...)

- Now that we are on equispaced modes, use a (F)DFT to reconstruct an approximation to $f \cdot \phi$ in physical space.
- Recover f by dividing out ϕ.
- This is typically implemented using a non-uniform FFT.

Why Do We Need Density Compensation?

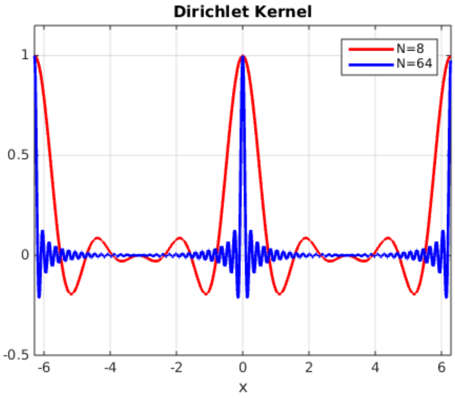

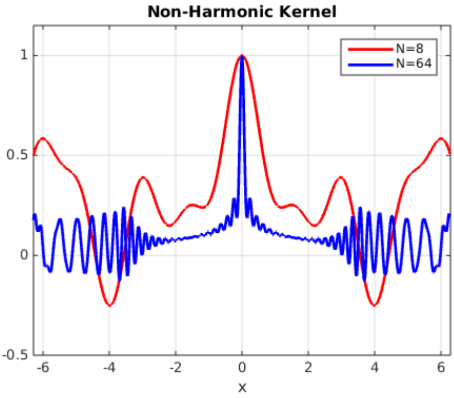

$$D_N(x) = \sum_{|k| \leq N} e^{ikx}$$

$$A_N(x) = \sum_{|k| \leq N} e^{i\omega_k x}$$

Why Do We Need Density Compensation?

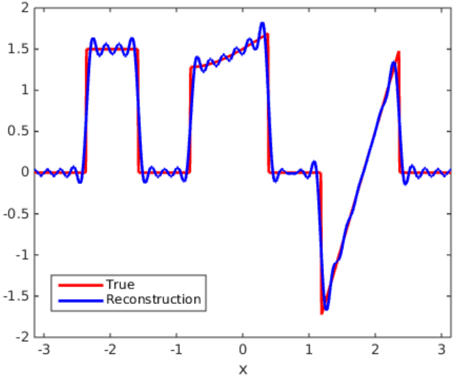

Uniform Samples

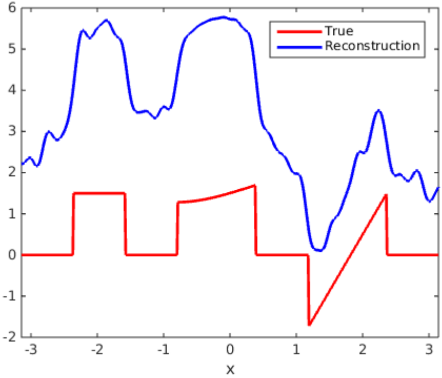

Quadratic Samples

Density Compensation – Examples

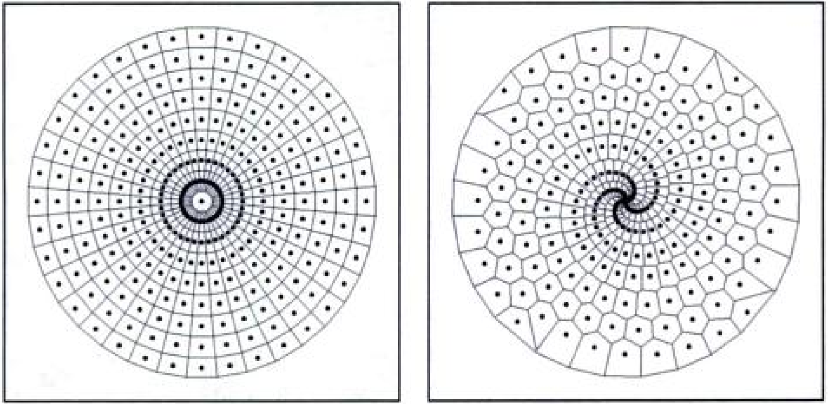

Figure : Voronoi Cells for Radial and Spiral Sampling[3]

[3] Modern Sampling Theory: Mathematics and Applications, eds. J. J. Benedetto, P. J.S.G. Ferreira, Birkhauser, 2001

Density Compensation – Examples

Choose $\boldsymbol{\alpha} = \{\alpha_k\}_{-N}^{N}$ such that[3]

$$\sum_{|k|\leq N} \alpha_k e^{i\omega_k x} \approx \begin{cases} 1 & x = 0 \\ 0 & \text{else} \end{cases}$$

Discretizing on an equispaced grid, we obtain the linear system of equations

$$D\boldsymbol{\alpha} = \mathbf{b},$$

where

- $D_{\ell,j} = e^{i\omega_\ell x_j}$ denotes the (non-harmonic) DFT matrix, and
- $\mathbf{b}$ denotes the desired point spread function (Dirac delta).

[3] See *Sampling density compensation in MRI: rationale and an iterative numerical solution*, Pipe JG, Menon P., Magn Reson Med. 1999 Jan;41(1): 179–86 for details and implementation.

Convolutional Gridding – Representative Reconstructions

Reconstruction from Polynomial (quadratic) samples.

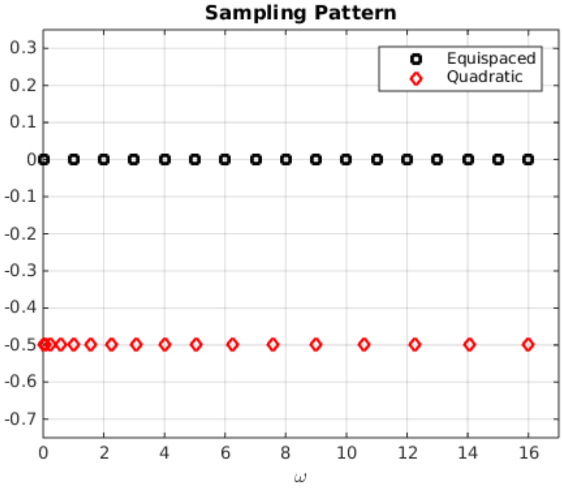

Convolutional Gridding – Representative Reconstructions

Reconstruction from Polynomial (quadratic) samples.

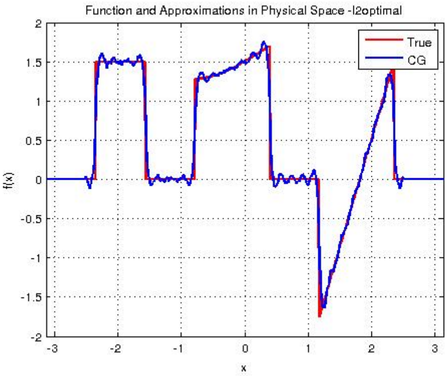

Reconstruction

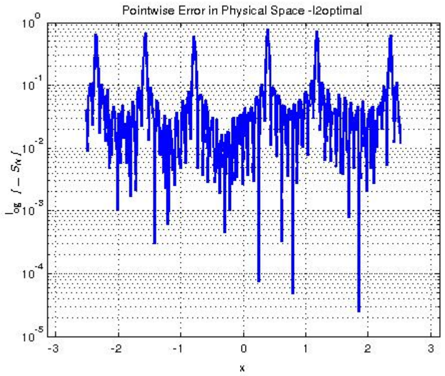

Reconstruction Error

Convolutional Gridding – Representative Reconstructions

Reconstruction from Spiral samples (Voronoi weights)[4]

True Image (Phantom)

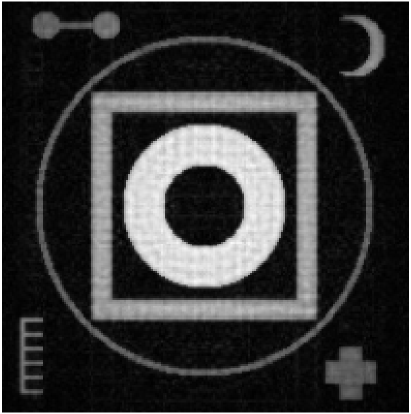

Reconstruction

[4] *A gridding algorithm for efficient density compensation of arbitrarily sampled Fourier-domain data*, W. Q. Malik et. al., Proc. IEEE Sarnoff Symp. Princeton, NJ, USA, Apr. 2005

Convolutional Gridding – Representative Reconstructions

Reconstruction from Spiral samples (Voronoi weights)[4]

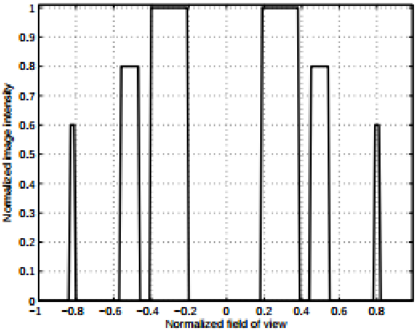

Cross Section

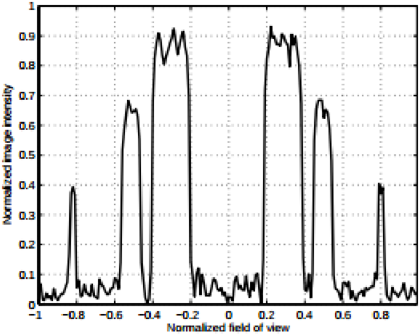

Reconstruction

[4] *A gridding algorithm for efficient density compensation of arbitrarily sampled Fourier-domain data*, W. Q. Malik et. al., Proc. IEEE Sarnoff Symp. Princeton, NJ, USA, Apr. 2005

Further Reading

- *A fast sinc function gridding algorithm for Fourier inversion in computer tomography*, J. O'Sullivan, IEEE Trans Med Imag 1985; MI–4:200–207.
- *Selection of a convolution function for Fourier inversion using gridding*, J. Jackson, C. Meyer, D. Nishimura, and A. Macovski, IEEE Trans Med Imag 1991; 10:473–478.
- *The gridding method for image reconstruction by Fourier transformation*, H. Schomberg and J. Timmer, IEEE Trans Med Imag 1995; 14:596–607.
- *Rapid gridding reconstruction with a minimal oversampling ratio*, P. Beatty, D. Nishimura, and J. Pauly, IEEE Trans Med Imag 2005; 24:799–808.

Non-Uniform Fourier Transforms (Greengard and Lee, 2004)

Non-uniform FFTs efficiently evaluate trigonometric sums of the form

$$\text{(Type I)} \quad F(k) = \frac{1}{N}\sum_{j=0}^{N-1} f_j e^{-ikx_j},\, x_j \in [0, 2\pi),\, k = -\frac{M}{2}, \ldots, \frac{M}{2} - 1.$$

$$\text{(Type II)} \quad f(x_j) = \sum_{k=-\frac{M}{2}}^{\frac{M}{2}-1} F(k) e^{ikx_j},\, x_j \in [0, 2\pi).$$

at a computational cost of $\mathcal{O}(N \log N + M)$.

Non-Uniform Fourier Transforms (Greengard and Lee, 2004)

The Type I FFT describes the Fourier coefficients of the function

$$f(x) = \sum_{j=0}^{N-1} f_j \delta(x - x_j)$$

viewed as a periodic function on $[0, 2\pi]$.

Note that f is not well resolved by a uniform mesh in x.

Non-Uniform Fourier Transforms (Greengard and Lee, 2004)

Instead, let us compute an approximation to f_τ defined as

$$f_\tau(x) = (f * g_\tau)(x) = \int_0^{2\pi} f(y) g_\tau(x-y) dy,$$

where $g_\tau(x)$ is a periodic one-dimensional heat kernel on $[0, 2\pi]$ given by

$$g_\tau(x) = \sum_{l=-\infty}^{\infty} e^{(x-2l\pi)^2/4\tau}.$$

f_τ may be approximated on a uniform grid using

$$f_\tau(2\pi m/M_r) = \sum_{j=0}^{N-1} f_j g_\tau(2\pi m/M_r - x_j).$$

Non-Uniform Fourier Transforms (Greengard and Lee, 2004)

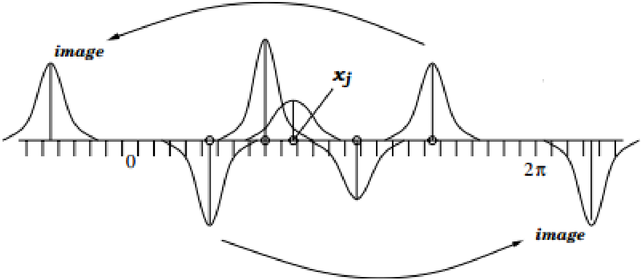

Figure : Non-Uniform FFT using Gaussian Window Functions[5]

f_τ is a 2π-periodic C^∞ function and can be well-resolved by a uniform mesh in x whose spacing is determined by τ.

[5]See *Accelerating the Nonuniform Fast Fourier Transform*, L. Greengard, J. Lee, SIAM Rev., Vol. 46, No. 3, pp. 443–454.

Non-Uniform Fourier Transforms (Greengard and Lee, 2004)

The Fourier coefficients of f_τ can be computed with high accuracy using a standard FFT on an oversampled grid. For example,

$$F_\tau(k) = \frac{1}{2\pi}\int_0^{2\pi} f_\tau(x)e^{-ikx}dx \approx \frac{1}{M_r}\sum_{m=0}^{M_r-1} f_\tau(2\pi m/M_r)e^{-ik2\pi m/M_r}.$$

We may then obtain $F(k)$ by a deconvolution; i.e.,

$$F(k) = \sqrt{\pi/\tau}e^{k^2\tau}F_\tau(k).$$

Typical parameters: $M_r = 2M, \tau = 12/M^2$. Gaussian spreading of each source to the nearest 24 points yields 12 digits of accuracy.

Other Implementations and Further Reading

- *Accelerating the Nonuniform Fast Fourier Transform*, L. Greengard and J. Lee, SIAM Rev., 46:3(2004), pp. 443–454.
- *Fast Fourier Transforms for Nonequispaced Data*, A. Dutt and V. Rokhlin, SIAM J. Sci. Comput., 14 (1993), pp. 1368–1393.
- *Nonuniform Fast Fourier Transforms using Min-Max Interpolation*, J. A. Fessler and B. P. Sutton, IEEE Trans. Signal Process., 51 (2003), pp. 560–574.
- *Fast Fourier Transforms for Nonequispaced Data: A Tutorial*, D. Potts, G. Steidl, and M. Tasche, in Modern Sampling Theory: Mathematics and Applications, J. J. Benedetto and P. Ferreira, eds., Appl. Numer. Harmon. Anal., Birkhauser, Boston, 2001, pp. 249–274.

Outline

Why are Edges Important?

- Edges are important descriptors of underlying features in a function.
- Edges are often necessary to perform operations such as segmentation and feature recognition.
- Edges may also be incorporated in function reconstruction schemes (for example, spectral re-projection methods)

Detecting Edges from Fourier Data

- Edge detection from Fourier data is non-trivial – it requires the estimation of *local* features from *global* data.
- Applying conventional edge detectors (Sobel, Prewitt, Canny ...) is not optimal – they can pick up Gibbs oscillations as edges.

Edge Detection from Non-Uniform Fourier Data

Two approaches (direct methods)

- Edge detection on re-sampled Fourier data

$$\hat{f}(\omega_k)_{\omega_k \notin \mathbb{Z}} \xrightarrow{\text{(B)URS}} \hat{f}(\ell)_{\ell \in \mathbb{Z}} \xrightarrow{\text{Edge Detection}} \text{Edges}$$

- Edge detection using convolutional gridding

$$\hat{f}(\omega_k)_{\omega_k \notin \mathbb{Z}} \xrightarrow{\text{Gridding}} (\hat{f} * \hat{\phi})(\ell)_{\ell \in \mathbb{Z}} \xrightarrow{\text{Edge Detection}} \text{Edges}$$

$$\hat{f}(\omega_k)_{\omega_k \notin \mathbb{Z}} \xrightarrow[\text{Special DCFs}]{\text{Gridding}} (\widehat{[f]} * \hat{\phi})(\ell)_{\ell \in \mathbb{Z}} \xrightarrow{\mathcal{F}^{-1}} \text{Edges}$$

Concentration Method (Gelb, Tadmor)

- Define the *jump function* as follows

$$[f](x) := f(x^+) - f(x^-)$$

$[f]$ identifies the singular support of f.

- Approximate the singular support of f using the *generalized conjugate partial Fourier sum*

$$S_N^\sigma[f](x) = i \sum_{k=-N}^{N} \hat{f}(k)\, \mathrm{sgn}(k)\, \sigma\left(\frac{|k|}{N}\right) e^{ikx}$$

- $\sigma_{k,N}(\eta) = \sigma\left(\frac{|k|}{N}\right)$ are known as *concentration factors*.

Concentration Method (Gelb, Tadmor)

- Define the *jump function* as follows

$$[f](x) := f(x^+) - f(x^-)$$

$[f]$ identifies the singular support of f.

- Approximate the singular support of f using the *generalized conjugate partial Fourier sum*

$$S_N^\sigma[f](x) = i \sum_{k=-N}^{N} \hat{f}(k)\, \mathrm{sgn}(k)\, \sigma\left(\frac{|k|}{N}\right) e^{ikx}$$

- $\sigma_{k,N}(\eta) = \sigma\left(\frac{|k|}{N}\right)$ are known as *concentration factors*.

Concentration Method (Gelb, Tadmor)

Admissibility conditions for σ:

1. $\displaystyle\sum_{k=1}^{N} \sigma\left(\frac{k}{N}\right)\sin(kx)$ is odd.

2. $\displaystyle\frac{\sigma_{k,N}(\eta)}{\eta} \in C^2(0,1)$

3. $\displaystyle\int_{\epsilon}^{1} \frac{\sigma_{k,N}(\eta)}{\eta} \longrightarrow -\pi, \quad \epsilon = \epsilon(N) > 0$ being small.

Concentration Method (Gelb, Tadmor)

Theorem (Concentration Property, (Tadmor, Zou))

Assume that $f(\cdot) \in BV[-\pi, \pi]$ is a piecewise C^2–smooth function and let $\sigma_{k,N}$ be an admissible concentration factor. Then, $S_N^\sigma[f](x)$ satisfies the concentration property

$$S_N^\sigma[f](x) = \begin{cases} \mathcal{O}\left(\frac{\log N}{N}\right), & d(x) \lesssim \frac{\log N}{N} \\ \mathcal{O}\left(\frac{\log N}{(Nd(x))^s}\right), & d(x) \gg \frac{1}{N}, \end{cases}$$

where $d(x)$ denotes the distance between x and the nearest jump discontinuity and $s = s_\sigma > 0$ depends on our choice of σ.

Concentration Factors

Factor	Expression
Trigonometric	$\sigma_T(\eta) = \frac{\pi \sin(\alpha\,\eta)}{Si(\alpha)}$ $Si(\alpha) = \int_0^{\alpha} \frac{\sin(x)}{x}\,dx$
Polynomial	$\sigma_P(\eta) = -p\,\pi\,\eta^p$ p is the order of the factor
Exponential	$\sigma_E(\eta) = C\eta \exp\left[\frac{1}{\alpha\,\eta\,(\eta-1)}\right]$ C - normalizing constant α - order $C = \frac{\pi}{\int_{\frac{1}{N}}^{1-\frac{1}{N}} \exp\left[\frac{1}{\alpha\,\tau\,(\tau-1)}\right] d\tau}$

Table : Examples of concentration factors

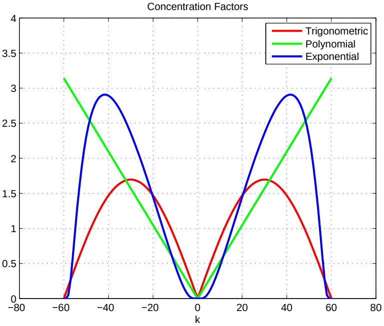

Figure :
Envelopes of Factors in k-space

Some Examples

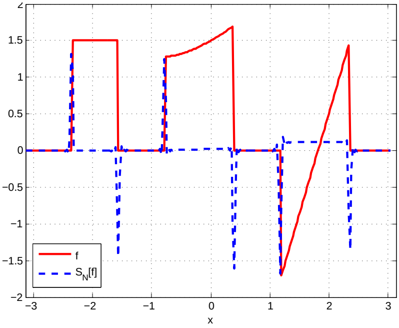

(a) Trigonometric Factor

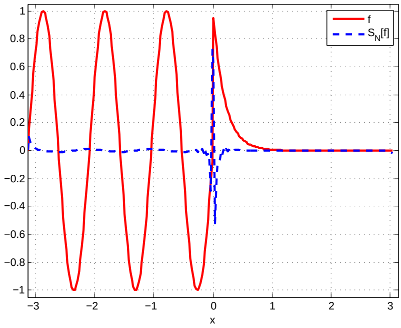

(b) Exponential Factor

Figure : Jump Function Approximation, $N = 128$

Statistical Formulation

Objective

Design a statistically optimal edge detector which accepts a noisy concentration sum approximation and returns a list of jump locations and jump values

Statistical Formulation

- This is a binary detection theoretic problem – is any given point in the domain an edge (hypothesis $\mathcal{H}_1$) or not (hypothesis $\mathcal{H}_0$)?
- The Neyman–Pearson lemma tells us that the statistically optimal construction in this case is a *correlation detector*, which computes correlations of $S_N^\sigma[f]$ with a template waveform .
- Uses a small number of measurements in a neighborhood of the given point[5]; for example, to see if the grid point x_0 is an edge, use

$$\mathbf{Y} = \begin{bmatrix} S_N^\sigma[f](x_0 - h) \\ S_N^\sigma[f](x_0) \\ S_N^\sigma[f](x_0 + h) \end{bmatrix}$$

[5] This will identify the closest grid point to an edge.

Statistical Formulation

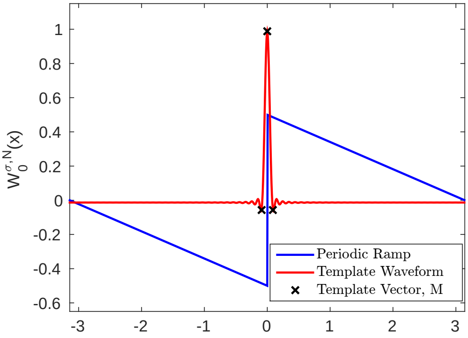

Figure : The Template Waveform and Template Vector

Resulting edge detector takes the form

$$\longrightarrow \mathcal{H}_1 : M^T C_{\mathbf{V}}^{-1} \mathbf{Y} > \gamma$$

- $C_{\mathbf{V}}$ is the covariance matrix (depends on the noise characteristics and stencil).
- γ is a threshold which controls the probability of correct detection.

Examples – Edge Detection with Noisy Fourier Data

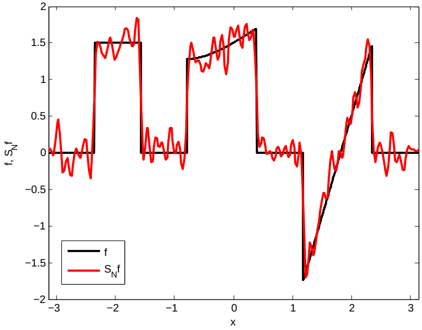

(a) Noisy Fourier Reconstruction

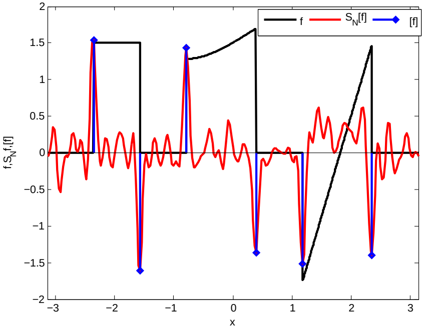

(b) Jump Detection

Figure : Edge Detection with Noisy Data, $N = 50, \rho = 0.02, 5-$point Trigonometric detector

Examples – Edge Detection with Noisy Fourier Data

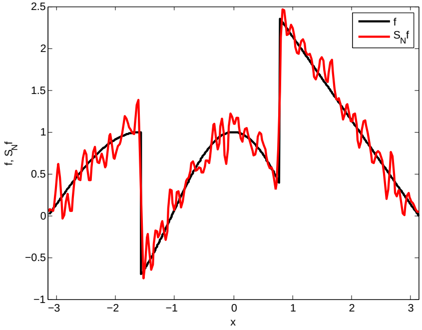

(a) Noisy Fourier Reconstruction

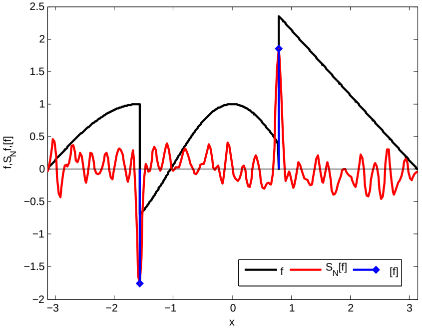

(b) Jump Detection

Figure : Edge Detection with Noisy Data, $N = 50, \rho = 0.02, 5-$point Trigonometric detector

Two Dimensional Extensions

For images, apply the method to each dimension separately

$$S_N^{\sigma}[f](x(\bar{y})) = i \sum_{l=-N}^{N} \mathsf{sgn}(l)\, \sigma\left(\frac{|l|}{N}\right) \sum_{k=-N}^{N} \hat{f}_{k,l}\, e^{i(kx+l\bar{y})}$$

(overbar represents the dimension held constant.)

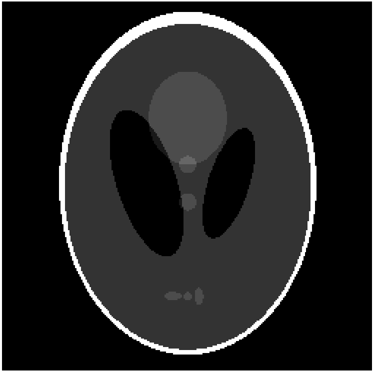

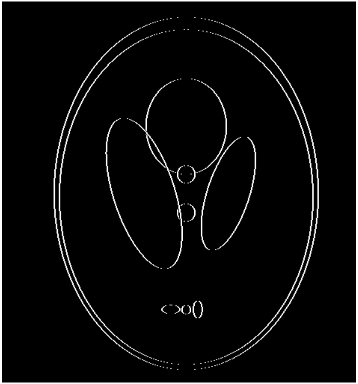

Two Dimensional Extensions

For images, apply the method to each dimension separately

$$S_N^\sigma[f](x(\bar{y})) = i \sum_{l=-N}^{N} \mathsf{sgn}(l)\, \sigma\left(\frac{|l|}{N}\right) \sum_{k=-N}^{N} \hat{f}_{k,l}\, e^{i(kx+l\bar{y})}$$

(overbar represents the dimension held constant.)

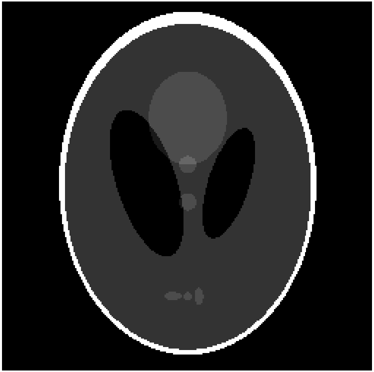

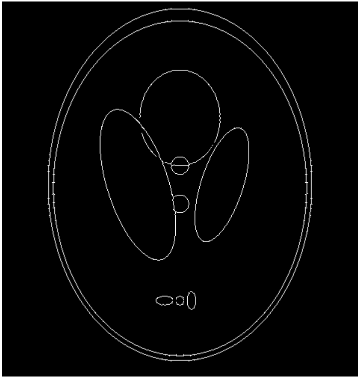

DCF Design for Edge Detection

Choose $\boldsymbol{\alpha} = \{\alpha_k\}_{-N}^{N}$ such that

$$\sum_{|k| \le N} \alpha_k e^{i\omega_k x} \approx \begin{cases} i \displaystyle\sum_{|\ell| \le M} \mathsf{sgn}(l)\sigma(|l|/N) e^{i\ell x} & |x| \le \pi \\ 0 & \text{else} \end{cases}$$

Discretizing on an equispaced grid, we obtain the linear system of equations

$$D\boldsymbol{\alpha} = \tilde{\mathbf{b}},$$

where

- D is the (non-harmonic) DFT matrix with $D_{\ell,j} = e^{i\omega_\ell x_j}$, and
- $\tilde{\mathbf{b}}$ is a vector containing the values of the generalized conjugate Dirichlet kernel on the equispaced grid.

Numerical Results

Jump Approximation and Corresponding Weights

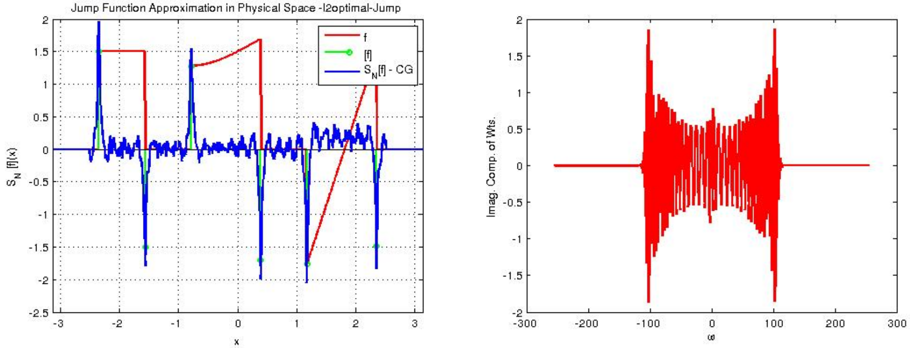

- ω_k logarithmically spaced
- $N = 256$ measurements
- Iterative weights solved using LSQR

Outline

Spectral Re-projection

- Spectral reprojection schemes were formulated to resolve the Gibbs phenomenon. They involve reconstructing the function using an alternate basis, Ψ (known as a Gibbs complementary basis).
- Reconstruction is performed using the rapidly converging series

$$f(x) \approx \sum_{l=0}^{m} c_l \psi_l(x), \quad \text{where} \quad c_l = \frac{\langle S_N f, \psi_l \rangle_w}{\|\psi_l\|_w^2}$$

- Reconstruction is performed in each smooth interval. Hence, we require jump discontinuity locations
- High frequency modes of f have exponentially small contributions on the low modes in the new basis

Gegenbauer Reconstruction – Representative Result

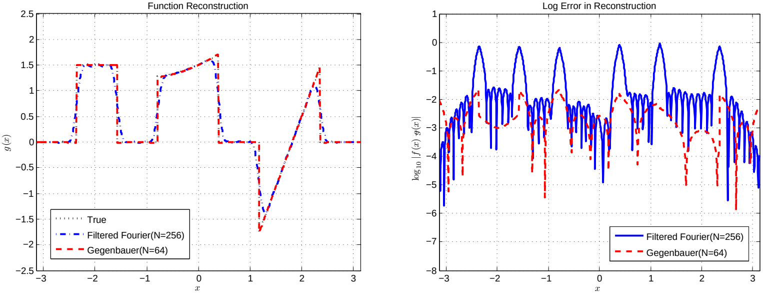

(e) Reconstruction (f) Reconstruction error

Figure : Gegenbauer reconstruction

- Filtered Fourier reconstruction uses 256 coefficients
- Gegenbauer reconstruction uses 64 coefficients
- Parameters in Gegenbauer Reconstruction - $m = 2, \lambda = 2$

Some Open Problems

1. Design of Density Compensation Factors and Gridding Windows
2. Exploiting piecewise-smooth structure and edges in reconstruction schemes
3. Parallel imaging
4. Dynamical sampling models and reconstruction schemes for motion corrected imaging